# Modeling the Distributed Physical Effects in the Intrinsic Base of SiGe HBTs Using Transmission Line Concepts

Germán Álvarez-Botero, Reydezel Torres-Torres and Roberto Murphy-Arteaga
*galvarez@inaoep.mx*, *reydezel@inaoep.mx*, *rmurphy@inaoep.mx*
National Institute for Astrophysics, Optics and Electronics (INAOE)
Deparment of Electronics
Tonantzintla, Puebla, Mexico

***Abstract*—The applicability of a transmission line model for representing the distributed high frequency effects in a SiGe HBT is demonstrated in this paper. In addition, the corresponding parameter extraction from S-parameter measurements is proposed, allowing to achieve excellent model-experiment correlation of the electrical behavior of the device's input characteristics up to 60 GHz.**

***Index Terms*—Heterojunction Bipolar Transistor, Distributed model, Parameter Extraction.**

## I. Introduction

SiGe BiCMOS technology provides an attractive solution to address the exigencies in performance of microwave integrated circuits for modern communication systems [1], [2]. In fact, recent papers predict that in the near future HBTs will be operating beyond the microwave frequency range [3]. However, even though there are recent papers dealing with the modeling of these devices up to some tens of gigahertz [4], [5], the corresponding accuracy is limited since the available models ignore the distributed nature of the structure of an HBT. This paper demonstrates that applying a rigorous Transmission Line analysis to the effects occurring in SiGe HBTs allows for a proper representation and physical model parameter extraction up to 60 GHz in a simple and straightforward way.

## II. Experiment

In order develop and verify the validity of the model proposed in this work, common-emitter SiGe HBTs were fabricated on p-type Si substrate in a $0.13\,\mu\mathrm{m}$ BiCMOS technology. Afterwards, on-wafer two-port measurements up to 60 GHz were taken on these devices using a vector network analyzer (VNA) and ground- signal-ground (GSG) coplanar RF probes with a $100\,\mu\mathrm{m}$ pitch. In this work, the HBTs were biased at $V_E$ = $V_C$ = 0 V in order to analyze the parasitics associated with the base-to-emitter junction. This particular bias is selected since the effect of the collector current is negligible in the small-signal model when the device is operating under this condition. The VNA was previously calibrated up to the probe tips, as shown in Fig. 1, using an off-wafer LRM (line-reflect-match) procedure, and an impedance-standard-substrate, establishing by this way a reference impedance of $50\,\Omega$.

Notice also in Fig. 1 that the DUT is embedded between pads and other interconnects to allow for the corresponding probing. In order to minimize the undesired effects associated with these interconnects, the pads are isolated from the substrate by using metal ground shields to reduce the coupling of the pads through the substrate. Nonetheless, the pad parasitic effects were also deembedded from the measurements by applying a two-step procedure and measurements collected from an 'open' and a 'short' dummy structures [6].

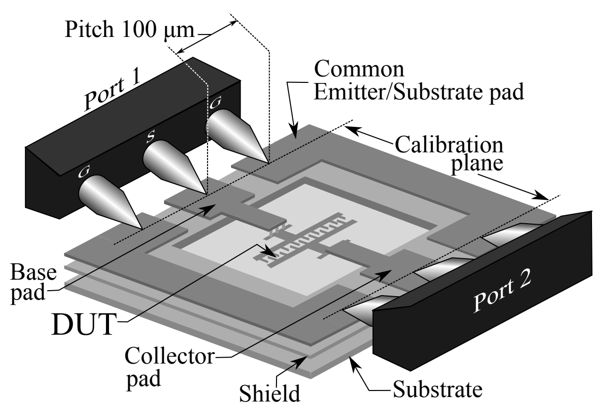


Fig. 1. Test structure pad configuration.

## III. Theory

Fig. 2 shows a simplified sketch illustrating how the HBT structure is represented using a distributed network, which considers the capacitances associated with the space charge layer at each side of the base region. These capacitances are referred to as base-emitter ($C_{be}$), and base-collector ($C_{bc}$) junction capacitances per unit length; the corresponding value depends on the doping profile and on the width of the associated depletion region. $r_{bi}$ is the intrinsic base resistance, which is a function of the bias conditions since the width of the space


ISBN 978-0-615-71756-2

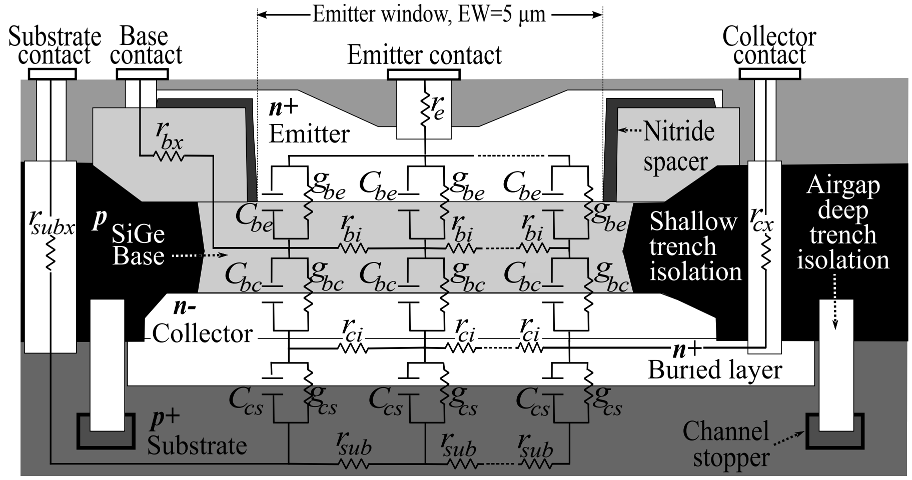


Fig. 2. Cross section of an HBT showing the allocation of the small-signal distributed equivalent circuit model.

charge layers determine the lateral resistance in the active base; $g_{be}$ and $g_{bc}$, are the dynamic base-emitter and base-collector conductances, respectively; the depletion capacitance formed at the bottom of the sub-collector-substrate junction is represented by means of $C_{sub}$, whereas the influence of the inner substrate resistance, and the additional resistances associated with the channel stopper and the substrate contacts are taken into account by $r_{sub}$.

Assuming common emitter/bulk configuration, and considering that high resistivity substrates are used in the fabrication process, the substrate effects can be neglected at some tens of gigahertz. Thus, the HBT equivalent circuit at $V_C = 0\ V$ can be rearranged to the form shown in Fig. 3 (a). A further simplification of the circuit can be carried out when short-circuiting the collector and emitter terminals (which is a common bias condition used for characterization purposes [7]). In this case, the circuit in Fig. 3 (b) can be obtained.

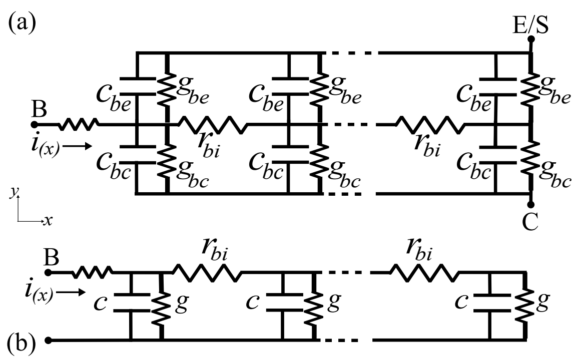


Fig. 3. Simplified models assuming (a) common emitter/substrate configuration at $V_C = 0\ V$, and (b) assumming that the HBT is terminated in short-circuit.

The model in Fig. 3 (b) represents the distributed nature of the base resistance and resembles an RCG transmission line. Hence, when the device is represented using this equivalent circuit, the distributed base resistance can be accurately analyzed at microwave frequencies using Transmission Line Theory concepts, which is the idea developed in this paper.

Solving the Telegraph Equations associated with the circuit in Fig. 3 (b) for the voltage and current along the base of the HBT results in:

$$v_{(x)} = \frac{V e^{j\omega t} \cosh(\gamma x)}{r_{bi} \cosh(\gamma x)} \tag{1}$$

$$i_{(x)} = \frac{-\gamma V e^{j\omega t} \sinh(\gamma x)}{r_{bi} \sinh(\gamma x)} \tag{2}$$

where $\gamma = \sqrt{r_{bi}(g + j\omega c)}$. Thus, the input impedance for the device can be written involving previous equations; after a mathematical simplification it yields:

$$Z_{in} = \frac{v_{(x)}}{i_{(x)}} = \frac{\coth\left(x r_{bi} \sqrt{\frac{g+j\omega c}{r_{bi}}}\right)}{\sqrt{\frac{g+j\omega c}{r_{bi}}}} \tag{3}$$

which is a Transmission Line Theory-based equation associated with the distributed base effects in an HBT. Thus, for an appropriate modeling of the HBT base terminal, this equation can be used together with the parameter extraction presented next.

## IV. Parameter extraction methodology

To determine the RGC parameters involved in (3), this expression can be simplified by representing $\coth(A + jB)$ by a Taylor series expansion:

$$\coth(A + jB) = \frac{\sum_{n=0}^{\infty} \frac{(A+jB)^{2n}}{(2n)!}}{\sum_{n=0}^{\infty} \frac{(A+jB)^{2n+1}}{(2n+1)!}} \tag{4}$$

and using two-terms in both the numerator and the denominator results in:

$$Z_{in} = \frac{xr_{bi}}{2} + \frac{1}{xg + j\omega xc} \tag{5}$$

This expression is equivalent to the equation for the short-circuit input impedance of the hybrid-$\pi$ circuit [8]. In fact, notice that this expression corresponds to a resistor ($xr_{bi}$) in series with the parallel connection of a capacitor ($xc$) and a conductor ($xg$), which is the typical circuit representation used for the base of an HBT. Thus, it is clear that (5) is a second-order approximation of (3) which can be applied at relative low frequencies. For high frequencies, however, it might be necessary to include higher order terms to obtain accurate results. This will be discused in the following section.

## V. Results and discussion

The input impedance associated with the circuit in Fig. 3 (b) corresponds to the HBT's $Z_{11}$ parameter, which can be written in terms of $r_{bi}$, $c$, and $g$ at relatively low frequencies when assuming $Z_{11} \approx Z_{in}$ (as defined in equation (6)). In this case, $Z_{11}$ can be written as:

$$Z_{11} = \frac{2g + r_{bi}c^2\omega^2}{2\omega^2 c^2} - j\frac{\omega c}{g^2 + c^2\omega^2} \tag{6}$$

From the real and imaginary parts of $Z_{11}$ the following expressions can be obtained:

$$\frac{-\omega}{\mathrm{Im}(Z_{11})} = \frac{g^2}{c} + c\omega^2 \tag{7}$$

$$2(\mathrm{Re}(Z_{11})\omega^2 - \frac{g}{c^2}) = r_{bi}\omega^2 \tag{8}$$

Then, after transforming the measured S-parameters of an HBT to Z-parameters, a linear regression of the experimental $-\omega/\mathrm{Im}(Z_{11})$ versus $\omega^2$ data can be performed. Using this regression, $c$ and $g$ can be respectively obtained from the corresponding slope and intercept with the abscises as shown in Fig. 4.

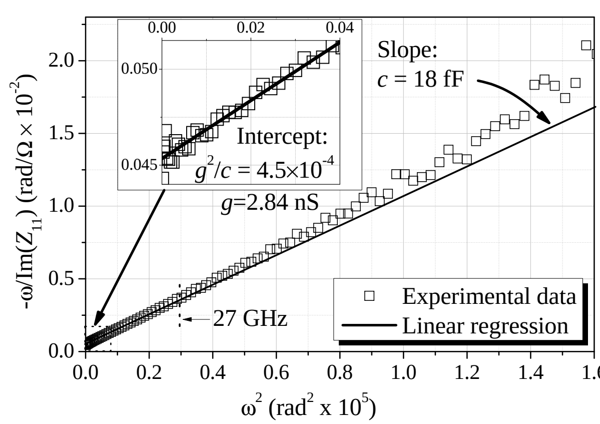


Fig. 4. Linear regression used to determine $g$ and $c$.

Once that $c$ and $g$ parameters are known, the linear regression of the experimental $2(\mathrm{Re}(Z_{11})\omega^2 - g/c^2)$ versus $\omega^2$ can be used to determine $r_{bi}$, as illustrated in Fig. 5.

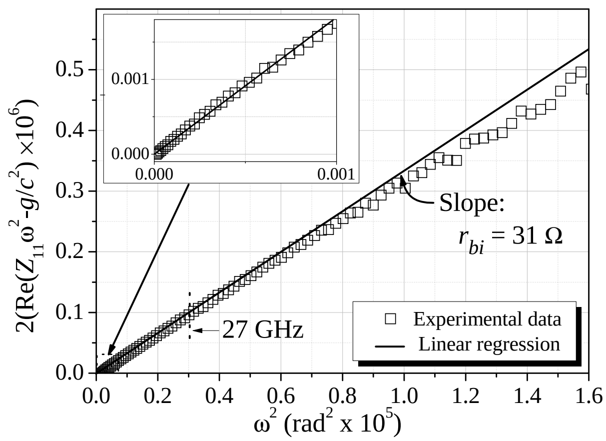


Fig. 5. Linear regression used to determine $r_{bi}$.

Notice the excellent linearity of the experimental data at relatively low frequencies (up to about 27 GHz) for both regressions. However, as the frequency rises, the two-term approximation losses validity and deviates from the experimental data, which means that more terms in the expansion expressed by (4) should be considered. Nonetheless, additional terms involve the very same parameters extracted at low frequencies, allowing to easily implement a more accurate model by including addends to the expansion given in (4). Alternatively, equation (3) can be directly used in the simulation to obtain the most accurate results that this model may yield.

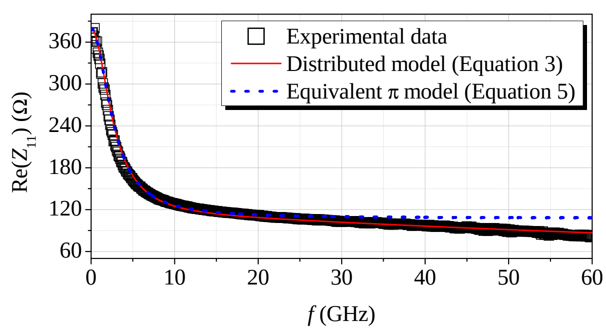


Fig. 6. Simulation-experiment correlation for the real part of $Z_{11}$.

Figs. 6 and 7 show that when using eq. (3) excellent model-experiment correlation is achieved when representing the complex $Z_{11}$ up to 60 GHz. In contrast, when using the simple and widely known $\pi$-model, the experimental $Z_{11}$ parameter data is appropriately reproduced only up to around 27 GHz.

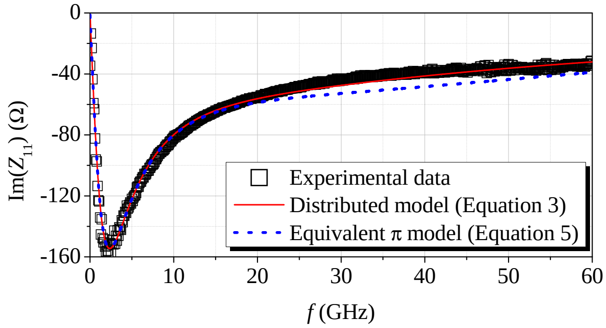


Fig. 7. Simulation-experiment correlation for the imaginary part of $Z_{11}$.

## VI. Conclusions

Commonly, the active base region effects are modeled for a small-signal operation using a traditional $\pi$-circuit model. However, through this study, the limitations of this model for high frequency representation of the base terminal effects in an HBT were evidenced. We have shown that modeling the HBT's base region using a lumped equivalent circuit is useful within a limited frequency range; outside this range the model becomes invalid. This is essentially because the distributed nature of the base effects is not considered.

Thus, through an analytical extraction method, proposed for determine the constitutive parameters of a transmission line model from S-parameters measurements, the frequency range where the simple $\pi$ model is valid has been determined for a SiGe HBT, obtaining that for frequencies beyond 27 GHz a most complete model is required for an accurate circuit behavior prediction. In this case, a very good simulation-experiment correlation for the input electrical characteristics of the HBT up to 60 GHz has been obtained using a complete distributed model.

## VII. Acknowledgements


The authors acknowledge IMEC, Leuven, Belgium for supplying the test structures. They also acknowledge the partial support of this project by CONACyT through Grant 83774-Y, and the scholarship to undertake doctoral studies number 213292.


## References


[1] M. Rudolph, "Compact HBT Modeling: Status and Challenges," in *Proceedings of the 2010 Microwave Symposium Digest (MTT)*, Anaheim, CA, 2010, pp. 1206–1209.

[2] T. Chen and J. Ma, "Advances in bipolar junction transistor modeling," in *Proceedings of the 10th IEEE International Conference on Solid-State and Integrated Circuit Technology*, Nov. 2010, pp. 1749–1752.

[3] A. Pawlak, M. Schroter, J. Krause, G. Wedel, and C. Jungemann, "On the feasibility of 500 GHz Silicon-Germanium HBTs," in *Proceedings of the International Conference on Simulation of Semiconductor Processes and Devices, SISPAD*, 2009, pp. 4–7.

[4] H. Taher, "Direct extraction technique of $\pi$-topology small-signal equivalent circuit model for Si/SiGe heterojunction bipolar transistor," *Microwave and Optical Technology Letters*, vol. 54, no. 3, pp. 584–589, 2012.

[5] M. J. Rodwell, M. Urteaga, T. Mathew, D. Scott, D. Mensa, Q. Lee, J. Guthrie, Y. Betser, S. C. Martin, R. P. Smith, S. Jaganathan, S. Krishnan, S. I. Long, R. Pullela, B. Agarwal, U. Bhattacharya, L. Samoska, and M. Dahlstrom, "Submicron Scaling of HBTs," *IEEE Transactions on Electron Devices*, vol. 48, no. 11, pp. 2606–2624, 2001.

[6] R. Torres-Torres, R. Murphy-Arteaga, and J. A. Reynoso-Hernández, "Analytical Model and Parameter Extraction to Account for the Pad Parasitics in RF-CMOS," *IEEE Transactions on Electron Devices*, vol. 52, no. 7, pp. 1335–1342, 2005.

[7] Y. Gobert, P. J. Tasker, and K. H. Bachem, "A Physical, Yet Simple, Small-Signal Equivalent Circuit for the Heterojunction Bipolar Transistor," *IEEE Transactions on Microwave Theory and Techniques*, vol. 45, no. 1, pp. 149–153, 1997.

[8] T.-R. Yang, J. M.-L. Tsai, C.-L. Ho, and R. Hu, "SiGe HBTs Small-Signal Pi Modeling," *IEEE Transactions on Microwave Theory and Techniques*, vol. 55, no. 7, pp. 1417–1424, Jul. 2007.